



Wu, H.-C., Park, Y.-K., Lin, J.-Y., Thanh, B. X., Jaree, A., Chen, W.-H., Lin, C.-H., [You, S.](#) and Lin, K.-Y. A. (2022) Oxidant-free and metal-free highly-selective catalytic production of vanillic aldehyde through activated carbon fiber-mediated aerobic oxidation. *[Journal of Cleaner Production](#)*, 375, 134141. (doi: [10.1016/j.jclepro.2022.134141](https://doi.org/10.1016/j.jclepro.2022.134141))

There may be differences between this version and the published version. You are advised to consult the published version if you wish to cite from it. <https://doi.org/10.1016/j.jclepro.2022.134141>

<https://eprints.gla.ac.uk/279688/>

Deposited on 28 October 2022

Enlighten – Research publications by members of the University of Glasgow  
<http://eprints.gla.ac.uk>

# Oxidant-Free and Metal-Free Highly-Selective Catalytic Production of Vanillic Aldehyde through Activated Carbon Fiber-mediated Aerobic Oxidation

*Hua-Chen Wu<sup>a</sup>, Young-Kwon Park<sup>b</sup>, Jia-Yin Lin<sup>a</sup>, Bui Xuan Thanh<sup>c</sup>, Attasak Jaree<sup>d</sup>,  
Wei-Hsin Chen<sup>e,f,g</sup>, Chia-Hua Lin<sup>h,\*</sup>, Siming You<sup>i</sup>, and Kun-Yi Andrew Lin<sup>a,\*</sup>*

<sup>a</sup>Department of Environmental Engineering & Innovation and Development Center of Sustainable Agriculture, National Chung Hsing University, 250 Kuo-Kuang Road, Taichung, Taiwan;

<sup>b</sup>School of Environmental Engineering, University of Seoul, Seoul 02504, Republic of Korea

<sup>c</sup>Faculty of Environment and Natural Resources, Ho Chi Minh City University of Technology, Ho Chi Minh City, 700000, Viet Nam

<sup>d</sup>Department of Chemical Engineering, Faculty of Engineering, Kasetsart University, Bangkok, Thailand

<sup>e</sup>Department of Aeronautics and Astronautics, National Cheng Kung University, Tainan 701, Taiwan

<sup>f</sup>Research Center for Smart Sustainable Circular Economy, Tunghai University, Taichung 407, Taiwan

<sup>g</sup>Department of Mechanical Engineering, National Chin-Yi University of Technology, Taichung 411, Taiwan

<sup>h</sup>Department of Biotechnology, National Formosa University, Yunlin 63208, Taiwan

<sup>i</sup>James Watt School of Engineering, University of Glasgow, Glasgow G12 8QQ, UK

\*Corresponding Authors. E-mail address: linky@nchu.edu.tw (K. Lin); vicchlin@nfu.edu.tw (C. Lin)

## Abstract

Typically, oxidizing agents (such as  $\text{H}_2\text{O}_2$ ) are necessitated for vanillic alcohol (VLA) conversion; nevertheless, intensive consumption of  $\text{H}_2\text{O}_2$  is required due to the stoichiometric chemistry, and metal catalysts are usually required to improve conversion of VLA by  $\text{H}_2\text{O}_2$ . Nevertheless, for pursuing the goal of sustainability, it would be highly desired to develop an oxidizing agent-free and metal-free process which can selectively oxidize VLA to vanillic aldehyde (VAE). The aim of this study is to propose activated carbon fiber (ACF) as a highly effective catalyst for VLA conversion to VAE without using metals and oxidizing agents. At 120 °C within 30 min, ACF could enable  $C_{\text{VLA}} = 100\%$  with  $S_{\text{VAE}} = 100\%$  without using metals/oxidants. The effect of radical scavengers and ESR analyses further reveal that the oxidation of VLA to VAE by ACF could be attributed to reactive oxygen species derived from ACF-mediated aerobic reactions.

**Keywords:** vanillic alcohol, vanillic aldehyde, carbon fiber, oxidation, biomass

## 1. Introduction

Biomass represent a key renewable source consisting of lignocellulosic substances, which can be depolymerized to generate various bio-derivatives [1-5]. Upgrading biomass derivatives to fuels and chemicals is an advantageous approach for transferring biomass to value-added products. Amid various bio-derivatives, vanillic alcohol (VLA) is a particularly promising bio-derivative because VLA can be obtained from lignin, and then converted to vanillin (VAE), a highly valuable product, which is extensively employed in numerous personal care products, perfumes, pharmaceuticals, and foods [6].

As conversion of VLA to VAE necessitates a particular oxidation of the alcohol group of VLA to an aldehyde group, it would be essential to establish a highly-selective oxidation process for converting VLA to VAE. Nowadays, the most traditional process for oxidation of VAL to VAE would be implemented by using oxidizing agents, such as  $H_2O_2$  [7-10]. Nonetheless, the stoichiometric oxidation of alcohol of VLA to VAE by  $H_2O_2$  would necessitate a large amount of  $H_2O_2$ . Besides, metal catalysts, and other energy inputs (e.g., light, ultrasound and heat) are also demanded for improving VLA oxidation by  $H_2O_2$  [7-11]. Nonetheless, conversion efficiencies of VLA to VAE by  $H_2O_2$ -involved techniques typically afford low conversion efficiencies and low selectivities because of over-oxidation of VLA or even decomposition of VLA [8, 10, 12, 13]. Therefore, such issues have limited large-scale and realistic operation of VLA oxidation by these traditional methods involved with metals, and oxidizing agents.

For pursuing the aim of sustainability, it would be imperative to establish a process which can convert VLA to VAE with a high conversion efficiency and a high selectivity but without usage of any metals and oxidizing agents. However, almost no such a study has been ever demonstrated. Thus, we report for the first time by using a carbon-based

material as a metal-free heterogeneous catalyst for oxidizing VLA without usage of any oxidizing agents. In particular, carbon fiber (CF) is selected because the fibrous shape of CF exhibits the high-aspect-ratio structure, allowing it to offer a high reactive surface. Besides, as VLA conversion to VAE is a thermo-chemical reaction, and CF is thermally conductive [14, 15], thereby serving as a promising catalyst for VLA oxidation. Moreover, since CF could be activated to maximize its surface area, and the activation process can also enable CF to possess more oxygenic functional groups, which are also reported to mediate oxidation reactions [16-19]. Therefore, activated CF (ACF) is also employed here for comparing with CF in VLA conversion to VAE in order to provide insights to elucidate property-activity relationships.

## **2. Experimental**

### **2.1 Materials**

Carbon fiber was obtained by carbonizing polyimide fiber (ca. 10  $\mu\text{m}$ , TITAN Company, Taiwan) in an atmosphere of  $\text{N}_2$ . The selection of polyimide fiber was because polyimide is a favorable carbon precursor, which would be converted into graphite fiber with higher thermal conductivity than other carbon fiber prepared using other polymers [20-22]. The resulting CF was then chemically activated using HCl followed by an additional thermal treatment based on reported protocols [23, 24]. In particular, 2 g of CF would be impregnated with 10 mL of HCl, and the piece of CF was then washed, and dried, followed by a heat treatment at 600  $^\circ\text{C}$  in an atmosphere of  $\text{N}_2$  for 6 hr to afford ACF.

Morphologies of CF and ACF were visualized by a scanning electron microscope (JOEL, Japan). XRD patterns of CF and ACF were characterized by an X-ray diffractometer (Bruker, USA), and their surface chemistry was analyzed by X-ray

photoelectron spectroscopy (XPS) (PHI 5000, ULVAC-PHI, Japan). Raman spectra of CF and ACF were obtained by a Raman spectrometer (Tokyo Instruments Inc., Japan). Textural properties of CF and ACF were determined by a volumetric gas adsorption analyzer (Anton Paar Nova Touch, Austria). The specific surface areas of ACF and CF were determined by examining N<sub>2</sub> sorption isotherms of ACF and CF using a volumetric gas adsorption analyzer. N<sub>2</sub> gas would be employed as an adsorbate, and ACF/CF were degassed for 10 h, and used for N<sub>2</sub> sorption at 77 K. At increasing pressure of N<sub>2</sub>, N<sub>2</sub> adsorbed to ACF/CF was quantified. The specific surface area would be then calculated based on the Brunauer-Emmett-Teller (BET) equation by sorption data acquired from the relatively pressure ( $P/P_0$ ) ranging from 0.05 to 0.3 [25]. In addition, pore size distributions of ACF/CF were determined by N<sub>2</sub> desorption isotherms of ACF/CF with the Barrett-Joyner-Halenda (BJH) method according to the modified Kelvin equation [26].

## **2.2 Catalytic VLA oxidation**

VLA oxidation would be implemented by batch experiments under either MW irradiation or traditional oven for examining effects of heating methods. Typically, VLA (40 mg) was introduced to the reactor containing 20 mL of isopropyl alcohol. Next, CF/ACF of 50 mg was added to the VLA solution, and the resulting mixture was then exposed to the ambient air (without pressurization of O<sub>2</sub>) and then heated at a desired temperature. Specifically, a Teflon-lined stainless-steel vessel (with an internal volume of 100 mL) would be employed in experiments heated by an electric oven. On the other hand, a Teflon-lined microwave vessel (an internal volume of 100 mL) would be used in experiments heated by a microwave oven. These aforementioned vessels would be sealed and screwed on tightly after loading reactants (including isopropyl

alcohol) for initiating the solvothermal reaction, in which the solvent would typically remain as a liquid in the testing temperature range of 40~120 °C.

The microwave apparatus used here is a high-performance microwave digestion system (ETHOS UP®, Milestone, Italy), which is one of the most advanced microwave systems in the market. In this microwave system, the temperature would be controlled (either at a ramping rate or at a fixed temperature) using an infrared sensor combined with an in-situ temperature sensor, which would be directly inserted into reaction media for precise temperature detection, and controlling by varying the energy input of the microwave system. With the infrared sensors and the in-situ temperature sensors, the reaction temperature can be verified, and ensured.

On the other hand, as solubilities of reactants in solvents would significantly influence reaction efficiencies, non-polar solvents, such as toluene, would be unfavorable, leading to very low conversions [27, 28]. On the other hand, among polar solvents, organic polar solvents have been also proven to exhibit much higher solubilities for VLA than inorganic polar solvents (e.g., H<sub>2</sub>O). Therefore, as a polar organic solvent, isopropyl alcohol has been validated as a suitable solvent for VLA conversion [27, 28].

The conversion of VLA was analyzed by HPLC with a UV-Vis detector and a reverse-phase C-18 column. Conversion of VLA to VAE was analyzed using the following equations [29]:

$$\text{VLA conversion } (C_{\text{VLA}}) = \text{VLA consumed} / \text{Total VLA } (\%) \quad (1)$$

$$\text{Selectivity for VAE } (S_{\text{VAE}}) = \text{VAE} / \text{VLA consumed } (\%) \quad (2)$$

$$\text{Yield for VAE } (Y_{\text{VAE}}) = \text{VLA conversion} \times \text{Selectivity for VAE } (\%) \quad (3)$$

### **3. Results and discussion:**

#### **3.1 Characterization of CF and ACF**

Firstly, the resultant CF and ACF were characterized for their appearances, and Fig. 1(a-c) reveal SEM images of CF, which exhibited a diameter of *ca.* 10  $\mu\text{m}$ . Fig. 1(b-c) indicating that the surface of CF was relatively smooth. On the other hand, Fig. 1(d-f) unveil the morphology of ACF, which exhibited the similar diameter but much roughened surface with noticeable small dents and holes. This demonstrates that the activation process had made the surface of ACF much more rugged to exhibit a relatively different surface texture.

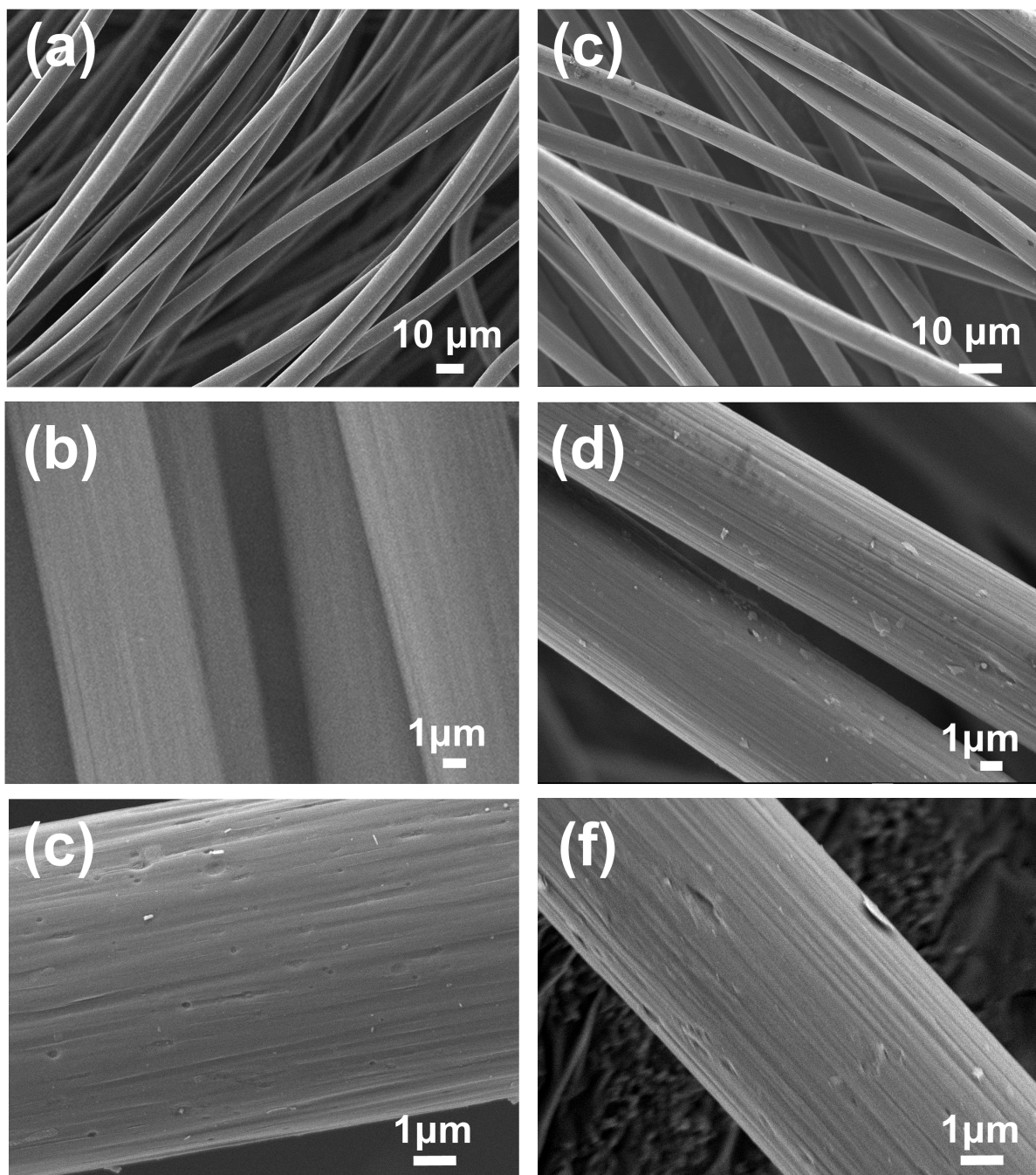


Fig. 1. Characterization of (a-c) carbon fiber, and (d-f) activated carbon fiber under different magnifications.

Fig. 2(a) then shows the XRD patterns of CF and ACE; both materials exhibited two noticeable peaks at 25.3 and 44.2°, attributed to the (002) and (100) planes in carbon (card #43-1104) [30]. Besides, the Raman spectra of CF and ACF revealed two typical peaks of carbonaceous materials located at 1353 and 1595 ( $\text{cm}^{-1}$ ) owing to the

disorderly-structured carbon (D band) and graphitic carbon (G band), respectively [30, 31]. These features confirmed that the as-prepared CF and ACF were certainly comprised of carbon without any notable amount of metals. This can be also validated by XPS analyses as shown in Fig. 2(c), in which the full-survey XPS scanning spectra of CF and ACF can be viewed, and noticeable signals of C, N, and O can be then detected without other significant signals of metals or any other elements. To further distinguish compositions of CF and ACF, elemental analyses of CF and ACF were then implemented, and elemental fractions of both materials were displayed in Fig 2(d). In both of materials, significant amounts of carbon with the presence of nitrogen, oxygen and hydrogen were observed. Moreover, one can note that ACF exhibited a much higher percentage of oxygen of 15.175% in contrast to that of 12.38% found in CF. This also suggests that the activation process caused ACF to possess more surficial oxygen groups.

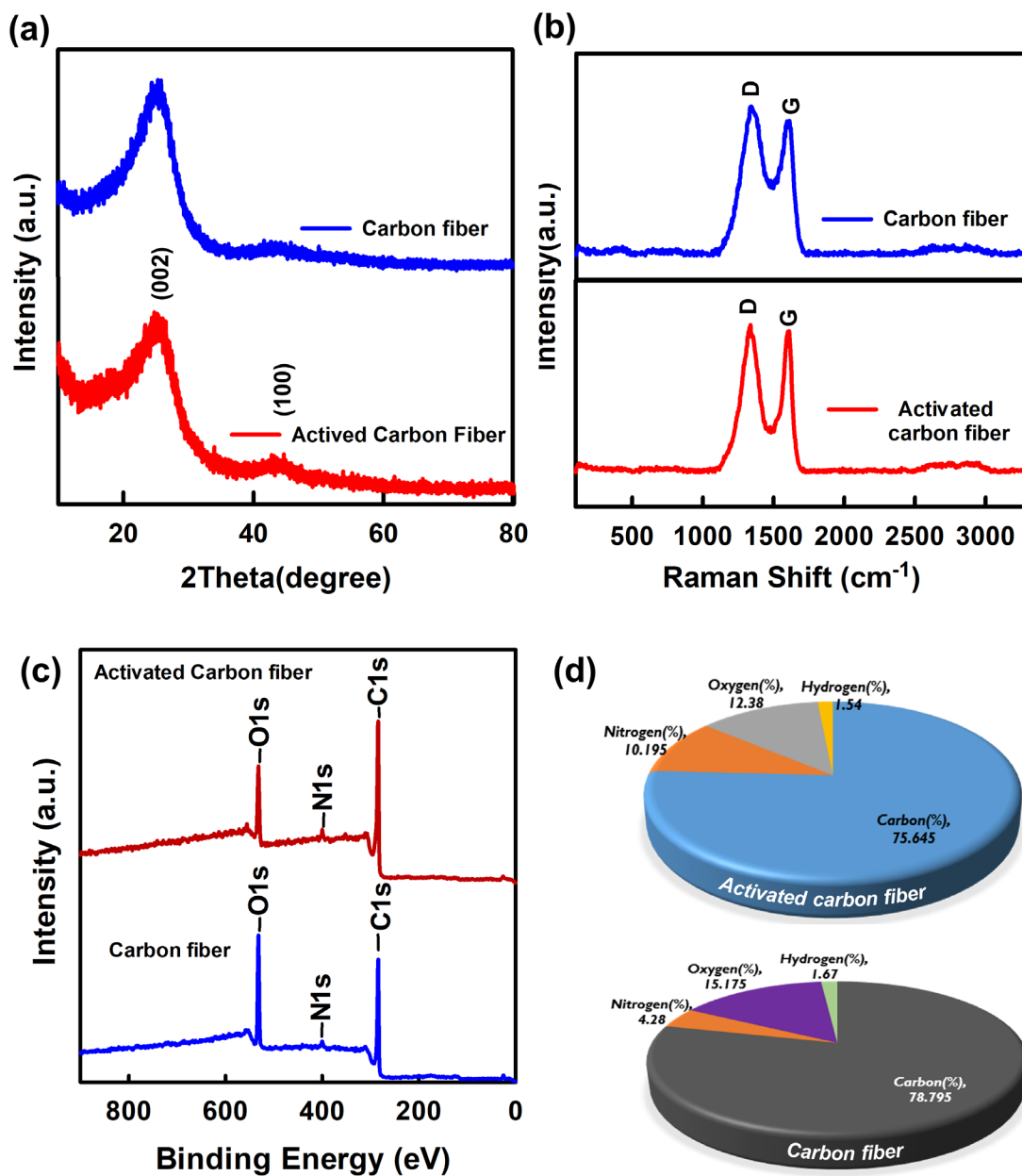


Fig. 2. Characterization of CF and ACF: (a) XRD pattern, (b) Raman, (c) chemical analysis by XPS, and (d) elemental analyses.

To further investigate surface chemistry of CF and ACF, their core-level spectra of C1s, O1s, and then N1s were then deconvoluted in Fig. 3. In particular, the C1s spectrum (Fig. 3(a)) reveals three peaks at 283.6, 284.8, and 288.0 eV, attributed to C-C, C-N and C=O, respectively [32]. Fig. 3(b) shows the O1s spectrum, in which two

peaks were revealed after deconvolution and attributed to C-O, and C=O [33]. Moreover, the N1s spectrum (Fig. 3(c)) was also deconvoluted to show two peaks at 398.5, and 400.5 eV corresponding to pyrrolic N species, and graphitic N species, respectively [34]. In the case of ACF, its C1s and N1s core-level spectra also were almost comparable to those seen in CF; however, its O1s spectrum was noticeably different from that of CF because a fraction of C=O was significantly augmented in ACF, suggesting that the activation process enabled ACF to possess more carbonyl groups on its surface.

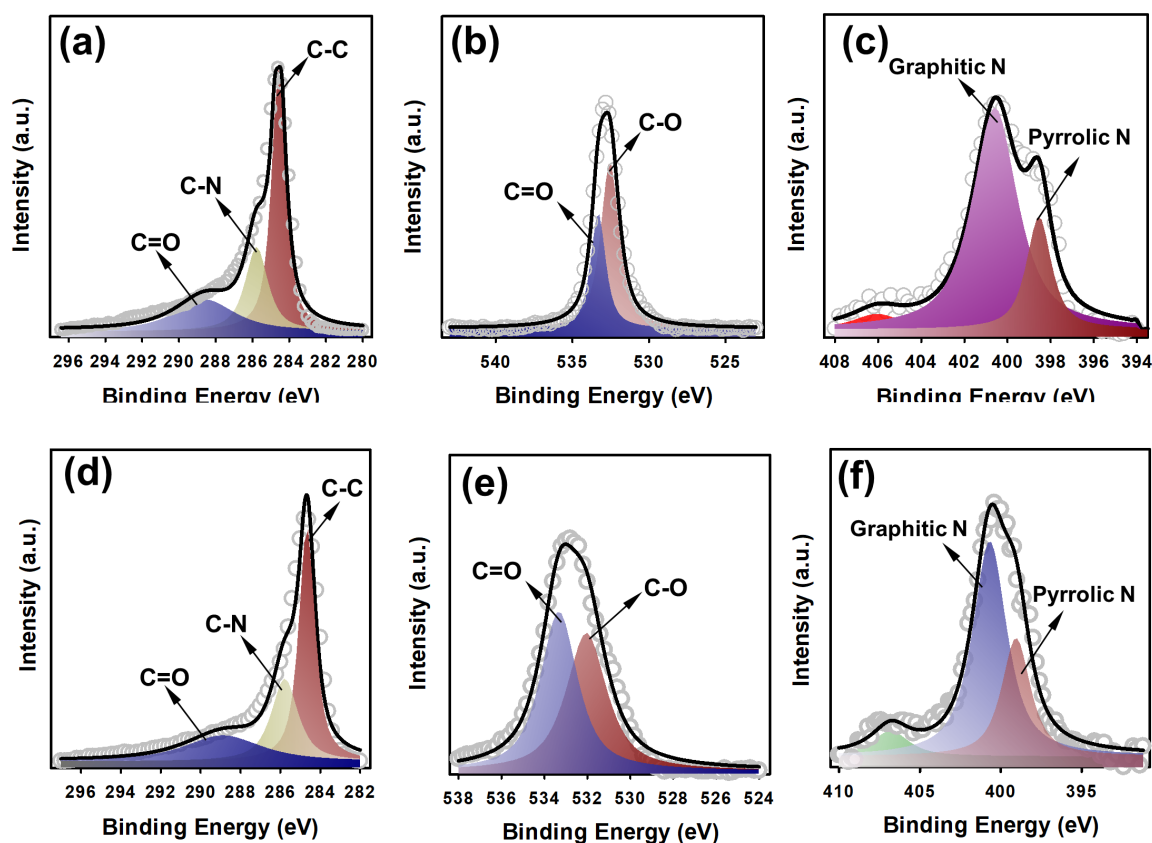


Fig. 3. XPS analysis of CF: (a) C1s, (b) O1s, and (c) N1s ; XPS analysis of ACF: (d) C1s, (e) O1s, and (f) N1s

Moreover, as CF and ACF exhibited noticeably different textures, their textural characteristics were then measured by determining their N<sub>2</sub> sorption/desorption isotherms (Fig. 4(a)). Essentially, both CF and ACF exhibited the IUPAC type I

isotherm; however, the N<sub>2</sub> sorption amount in ACF was considerably greater than that in CF, causing ACF to possess a much larger surface area of 902 m<sup>2</sup>/g than that of CF (198 m<sup>2</sup>/g). Moreover, pore size distributions of CF and ACF were also displayed in Fig. 4(b), indicating that ACF certainly possessed much more pores than CF as the total pore volume of ACF was 0.030, whereas the total pore volume of CF was merely 0.006 cm<sup>3</sup>/g. The higher surface area of ACF might be ascribed to the much more rugged surface of ACF as observed in a number of previous studies [24, 35]. These characterizations of CF and ACF certainly revealed that ACF and CF possessed noticeably distinct surficial and textural properties, which shall influence their activities during catalytic reactions.

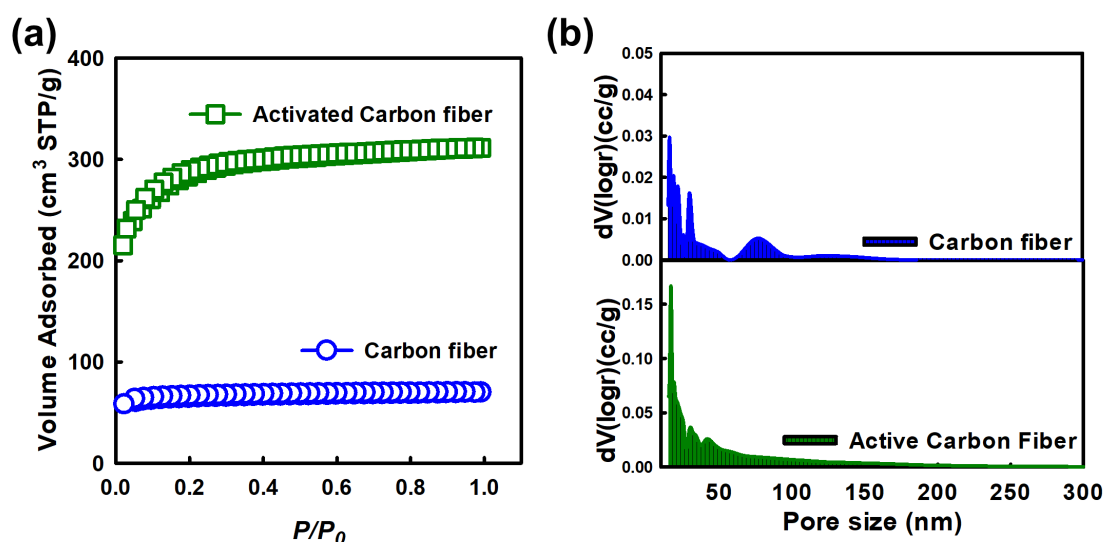


Fig. 4. Textural properties of CF and ACF: (a) N<sub>2</sub> sorption isotherm, and (b) pore size distribution

### 3.2 Catalytic conversion of vanillic alcohol

As VLA conversion to VAE is a thermo-chemical reaction, it was critical to investigate VLA conversion under different heated environments especially because carbon is a thermally-conductive material [14, 15, 36]. Therefore, traditional oven heating and microwave heating were then chosen for comparing their capabilities for thermal

processes. Prior to investigating VLA conversion in the presence of catalysts, it would be essential to examine how VLA would react during heating processes. Thus, Fig. 5 firstly shows VLA conversion under either traditional oven and microwave heating alone in the absence of any catalysts/oxidants. As oven heating was adopted, almost no VLA was consumed/converted.

On the other hand, as microwave was used, a very insignificant amount of VLA was consumed; however, no product was ever detected. These results indicate that VLA could not be converted to VAE directly by heating using either oven or microwave. Next, it would be also necessary to investigate if heating combined with oxidants would convert VLA to VAE. Since  $H_2O_2$  is the most typical oxidant for conversion of VLA [7, 11],  $H_2O_2$  was then adopted here for VLA conversion. When  $H_2O_2$  was combined with oven heating, a noticeably amount of VLA was converted ( $\sim 15.8\%$ ), and, a notable amount of VAE was detected ( $\sim 9.2\%$ ), demonstrating that the presence of oxidant could oxidize VLA and transform it to VAE. Nonetheless, the selectivity for VAE was relatively low as 58% as a noticeable amount of VAC could be also detected possibly due to over-oxidation and non-selective oxidation by  $H_2O_2$  [8, 9, 11, 37].

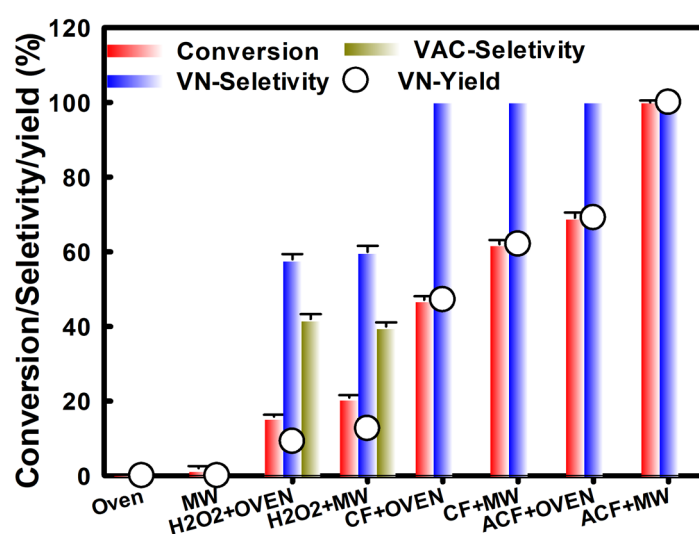


Fig. 5. VLA conversion by various methods ( $T = 120\text{ }^{\circ}\text{C}$ ,  $t = 30\text{ min}$ ).

On the other hand, when H<sub>2</sub>O<sub>2</sub> was combined with microwave heating, an even higher VLA conversion ( $C_{VLA}$ ) of 21.0% was afforded with a slightly higher VAE yield ( $Y_{VAE}$ ) of 12.6%. This indicates that VLA conversion to VAE could be achieved by H<sub>2</sub>O<sub>2</sub> and enhanced under microwave heating as microwave offers heat more quickly and homogeneously [38-41]. However,  $C_{VLA}$  by H<sub>2</sub>O<sub>2</sub>/microwave was still very low and a noticeable amount of VAC could be still produced due to the over-oxidation/non-selective oxidation by H<sub>2</sub>O<sub>2</sub>. These comparisons indicated that oxidants are critical for conventional VLA conversion; however, the conversion efficiency was unsatisfactory.

On the other hand, when CF alone (without any oxidants) was introduced to a VLA solution under traditional oven heating, interestingly, a huge fraction of VLA was converted ( $C_{VLA} = 47.1\%$ ). More critically, a significantly high amount of VAE could be observed with no VAC, leading to a superior selectivity for VAE (i.e., 100%). In the case of microwave heating,  $C_{VLA}$  could be even higher at 62.0%, and  $S_{VAE}$  was also 100%. These results indicate that CF alone can act as a catalyst for converting VLA to VAE, and an ultra-high selectivity of 100% for VAE can be achieved without production of VAC as well as other side products. Moreover, when ACF alone was adopted under oven heating, VLA was also successfully converted and a higher conversion of 69.1% was reached with a  $S_{VAE} = 100\%$ . Furthermore, when ACF was employed under microwave heating, a significantly higher  $C_{VLA} = 100\%$  with  $S_{VAE} = 100\%$  was obtained. These results validate that ACF alone could also oxidize VLA and convert VLA to VAE, and ACF seemed to enable a much higher VLA conversion than CF. Especially, ACF under microwave heating can completely convert VLA to VAE at 120 °C within 30 min.

The comparisons of VLA conversion between oven heating and microwave irradiation also suggested that microwave would be an even more efficient heating method because microwave typically enables faster and stronger heat from the internal region of catalysts [38-41]. Moreover, carbonaceous fiber has been also proven as a superior material for absorbing microwave [42]. Therefore, VLA conversion under microwave heating could be much enhanced because CF/ACF would effectively absorb microwave irradiation to reach the favorable temperature much more quickly, and uniformly [43, 44].

Moreover, in comparison to the reported conversion efficiencies of VLA to VAE (Table 1), such a high conversion efficiency with the ultra-high selectivity of VLA conversion to VAE by ACF was unprecedented and extremely promising.

**Table 1. VLA conversion by various methods involved with H<sub>2</sub>O<sub>2</sub>**

<i>Catalyst</i>	<i>Oxidant</i>	<i>Temp.(°C)</i>	<i>VLA Con. (%)</i>	<i>VAE Sel.(%)</i>	<i>VAE Yield(%)</i>	<i>Ref.</i>
<b>Activated Carbon fiber</b>	-	<b>120</b>	<b>100</b>	<b>100</b>	<b>100</b>	<b>This study</b>
CuO/MgAl <sub>2</sub> O <sub>4</sub>	H <sub>2</sub> O <sub>2</sub>	90	67	74	49.58	[45]
CuO/MgFe <sub>2</sub> O <sub>4</sub>			53	46	24.38	
MnCl <sub>2</sub>	H <sub>2</sub> O <sub>2</sub>	75	38	19	7.2	[13]
	H <sub>2</sub> O <sub>2</sub>	75	28	5	1.4	
	H <sub>2</sub> O <sub>2</sub>	80	89.6	49.4	44.3	
CrCl <sub>3</sub>	H <sub>2</sub> O <sub>2</sub>	80	94.2	60.6	57.1	
CoCl <sub>2</sub>	H <sub>2</sub> O <sub>2</sub>	80	48.1	33.9	16.3	
FeMCM-41(100)	H <sub>2</sub> O <sub>2</sub>	60	85	82	69.7	[3]
Co <sub>3</sub> O <sub>4</sub>	H <sub>2</sub> O <sub>2</sub>	75	38	50	19.0	[46]
Cu–Mn mixed oxide	H <sub>2</sub> O <sub>2</sub>	85	94	99	93.0	[47]
Cu <sub>3</sub> TiO <sub>4</sub> -TiO <sub>2</sub>	H <sub>2</sub> O <sub>2</sub>	85	66	71	46.9	[48]

### 3.3 Effect of temperature and time on conversion of vanillic alcohol

As CF and ACF were validated to catalyze VLA conversion to VAE, and microwave heating was validated to enhance VLA conversion, it would be essential to further investigate effects of temperature and reaction time on VLA conversion. Fig. 6(a) firstly reveals the effect of temperature on VLA conversion using CF under microwave heating. At a relatively low temperature of 40 °C, a relatively low amount of VLA could be still converted and successfully transformed to VAE (i.e.,  $C_{VLA} = 10.3\%$  and  $S_{VAE} = 100\%$ ). When the temperature increased to 60 °C,  $C_{VLA}$  also increased to 28.1% with  $S_{VAE} = 100\%$ , indicating that CF could also convert VLA to VAE even at relatively low temperatures. Once the temperature increased to 80, 100, and 120°C,  $C_{VLA}$  could then increase to 38.2, 53.4 and 62.0%, respectively, confirming the enhancing effect of higher temperatures.

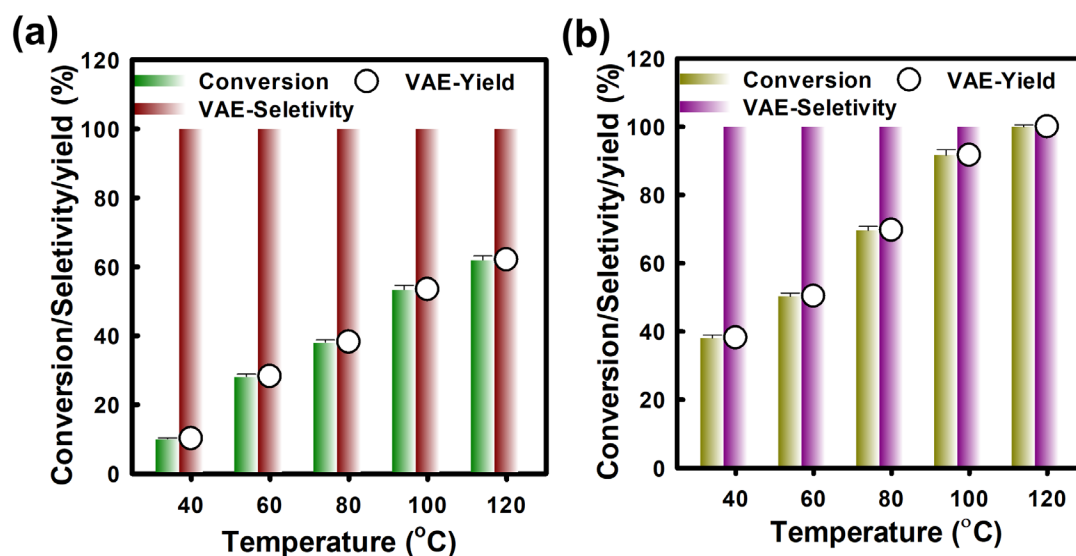


Fig. 6. Effect of temperature on VLA conversion by (a) CF and (b) ACF (t = 30 min).

On the other hand, in the case of ACF, VLA could be also successfully converted to VAE with  $C_{VLA} = 38.2\%$  and  $S_{VAE} = 100\%$  at 40 °C. When temperature increased gradually to 60 °C,  $C_{VLA}$  further increased to 50.3% with  $S_{VAE} = 100\%$ . Once

temperature ramped to 80, 100, and 120 °C, the corresponding  $C_{VLA}$  increased to 69.7, 91.6 and 100%, respectively. These results also demonstrate that temperature was a key factor, and VLA could be already converted to VAE at relatively low temperature, whereas a relatively high temperature would enable almost complete conversion of VLA to VAE by ACF. Thus, 120 °C was then chosen as a reference temperature for studying other effects.

Additionally, the effect of reaction time was also investigated in Fig. 7 by changing reaction time from a very brief time of 15 min to 120 min. In the case of CF, within 15 min at 120 °C, VLA could be successfully converted to VAE with  $C_{VLA}=46.5$  ( $S_{VAE} = 100\%$ ). This validates that even such a short time of 15 min, CF could still convert VLA to VAE. When a relatively longer time of 30 min was used, a much higher  $C_{VLA} = 62.7\%$  with  $S_{VAE} = 100\%$  was reached. Once the reaction time was extended to 60, 90 and 120 min,  $C_{VLA}$  was then correspondingly increased to 86.7%, 96.7%, and 98.0%, respectively. These results indicate that the reaction time as short as 15 min was still capable of converting VLA to VAE, and a longer reaction duration would significantly enhance VLA conversion to VAE.

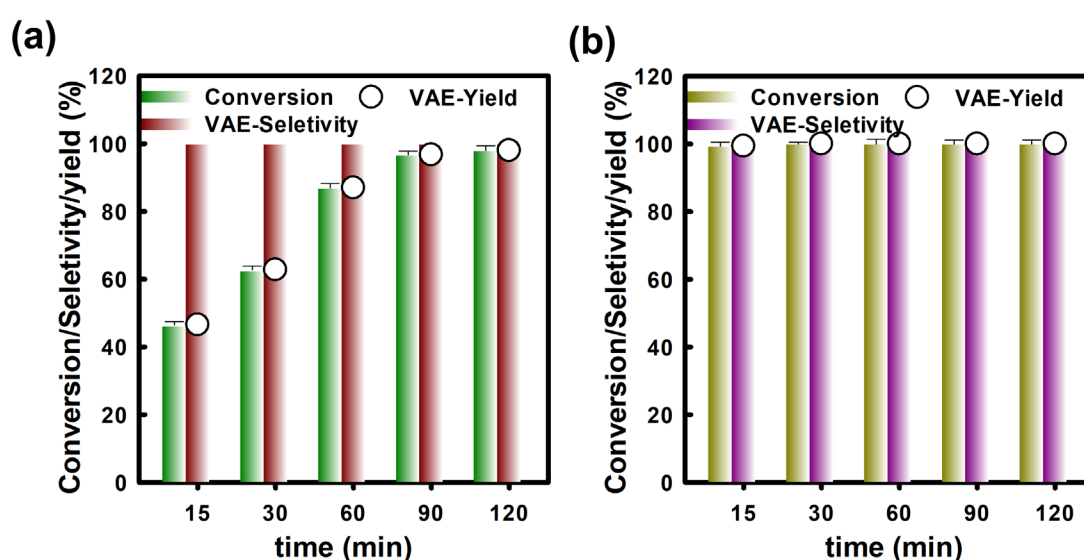


Fig. 7. Effect of reaction time on VLA conversion by (a) CF and (b) ACF (T = 120 °C).

On the other hand, similar results can be observed in the case of ACF. When the reaction time was as short as 15 min,  $C_{VLA}$  had reached 99.4% with  $S_{VAE} = 100\%$ , indicating that ACF possessed a very strong catalytic activity for conversing VLA to VAE even within such a short period. Once the reaction time increased to 30 min,  $C_{VLA}$  had increased to 100%. When the time was further extended to 60, 90 and 120 min,  $C_{VLA}$  could be maintained as 100%, and more importantly,  $S_{VAE}$  was consistently remained as 100%. To compare the kinetics of VAE yield using these two heating methods, the pseudo first order rate law:  $\ln(C_t/C_0) = e^{-kt}$  would be adopted as this rate law has been reported for VLA conversion [49]. The corresponding  $k$  for the VAE yield by CF and ACF were 0.040, and 0.365  $\text{min}^{-1}$ , respectively, indicating that the MW system would offer a much faster reaction kinetics for converting VLA to VAE. These results certified that ACF was a promising catalyst to ultra-selectively convert VLA to VAE without over-oxidation/non-selective oxidation. The significantly higher surface area of ACF (902  $\text{m}^2/\text{g}$  versus 198  $\text{m}^2/\text{g}$  of CF) might allow ACF to provide much more reactive sites for catalyzing oxidation of VLA, thereby leading to such a higher conversion efficiency.

### 3.4 Recyclability of ACF for conversion of VLA

Moreover, it was crucial to examine whether CF or ACF could be reused for VLA conversion as CF/ACF was proposed as a heterogeneous catalyst. Since ACF had successfully achieve  $C_{VLA} = 100\%$  with  $S_{VAE} = 100\%$  within 30 min at 120 °C, the recyclability of CF/ACF was tested using a reaction time of 30 min. Fig. 8(a) firstly shows five consecutive cycles of VLA conversion by CF, and CF could still oxidize VLA and convert it to VAE, and  $C_{VLA}$  could be remained  $> 60\%$  with  $S_{VAE} = 100\%$

over the five cycles. On the other hand, the recyclability of ACF was also tested over five cycles, and its  $C_{VLA}$  could still maintain as 100% with a consistent  $S_{VAE} = 100\%$  without noticeable reduction. Fig. S1 further reveals the XRD pattern of the used ACF, which was comparable to that of the pristine ACF. Besides, the morphology of the used ACF was also similar to those of the pristine ACF as the fibrous structure of ACF was preserved (Fig. S2), and its surface remained rugged without noticeable decomposition. Thus, the used ACF could still exhibit a relatively high surface area of  $892 \text{ m}^2/\text{g}$  with nanoscale porosity (Fig. S3). These results suggest that ACF remained intact without significant changes after the multiple-cyclic VLA conversion. These results confirm that ACF exhibited a very steady and effective catalytic activity for consecutive conversion of VLA to VAE, and no metal/oxidant was required to enable the recyclability of CF for VLA conversion.

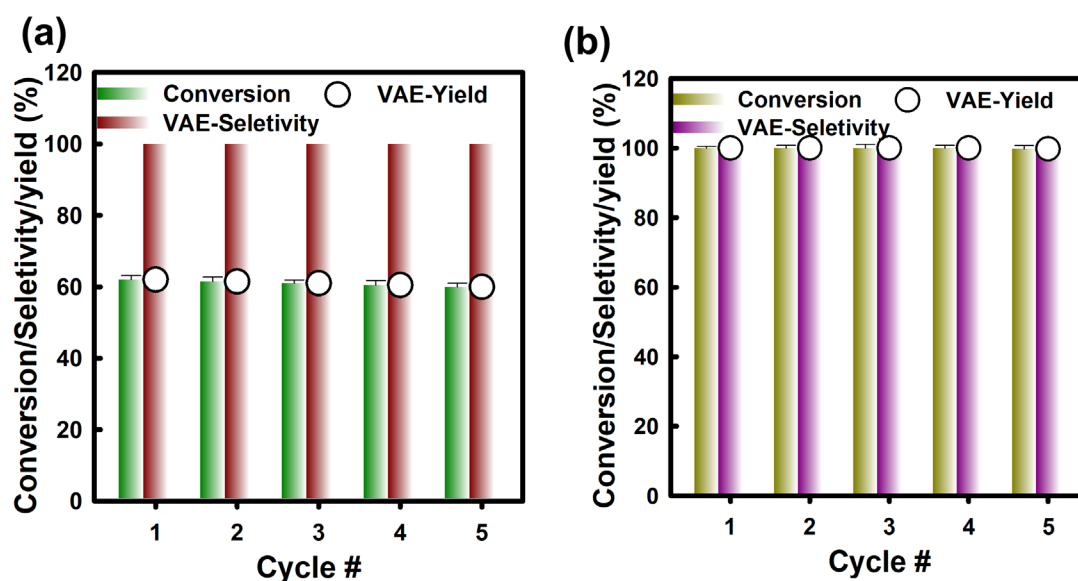


Fig. 8. Recyclability of (a) CF and (b) ACF for VLA conversion to VAE ( $T = 120 \text{ }^\circ\text{C}$ ,  $t = 30 \text{ min}$ ).

### 3.4 Possible mechanisms of conversion of vanillic alcohol by ACF

As ACF (and CF) successfully catalyzed conversion of VLA to VAE with the very high selectivity, it would be important to probe into the mechanism for VLA oxidation by ACF. Since ACF/CF is a carbon-based material, carbonaceous substances have been confirmed to act as catalysts for oxidation reactions related to several reactive oxygen species (ROS) (such as free radicals and singlet oxygen) [50]. To validate the occurrence of ROS generated from ACF/CF, the effect of radical scavenger on VLA conversion was then investigated. Specifically, tert-butanol was chosen as a probing agent for detecting the occurrence of hydroxyl radical ( $\cdot\text{OH}$ ). Fig. 9(a) displays VLA conversion by CF at 120 °C after 30 min in the presence of tert-butanol. Nonetheless, no notable reduction in YVAE was observed in both cases of ACF and CF, signifying that  $\cdot\text{OH}$  seemed not the principle ROS for VLA oxidation to VAE. Furthermore,  $\text{NaN}_3$  was then selected as a probing agent for detecting the occurrence of singlet oxygen. After adding  $\text{NaN}_3$  into VLA conversion by ACF/CF, YVAE was slightly decreased, suggesting that the addition of  $\text{NaN}_3$  might suppress VLA conversion to VAE and singlet oxygen shall exist in ACF-mediated oxidation of VLA.

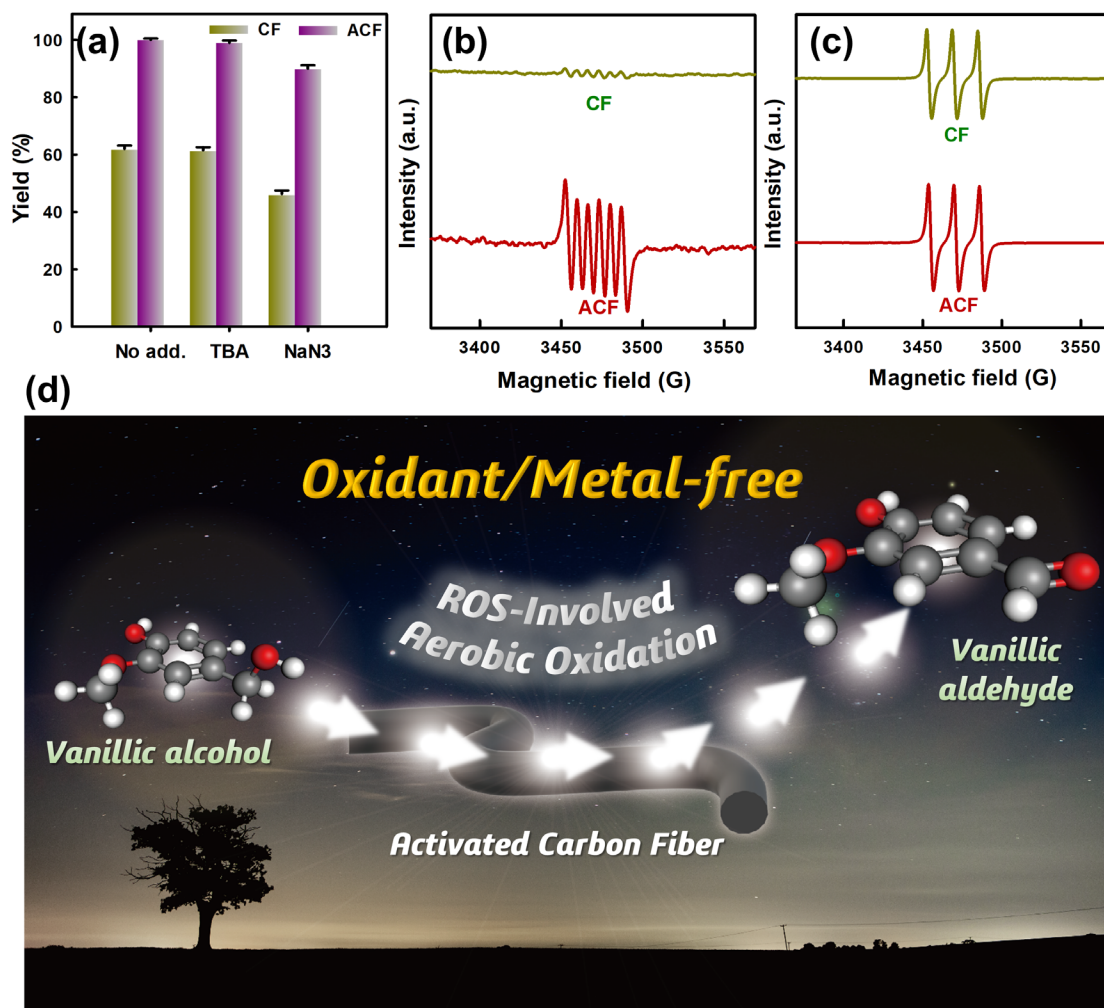


Fig. 9. (a) Effects of radical scavengers on VLA conversion by CF and ACF ( $T = 120\text{ }^{\circ}\text{C}$ ,  $t = 30\text{ min}$ ), (b) ESR analysis using DMPO, and (c) using TEMP; (d) illustration of VLA conversion to VAE by ACF.

To further examine the contribution of ROS to VLA oxidation, electron spin resonance (ESR) was then employed by using 5,5-Dimethyl-1-pyrroline N-oxide (DMPO) as a radical-trapping agent for determining  $\cdot\text{OH}$  or other radicals. Fig. 9(b) reveals that ACF exhibited a noticeable signal of sextet pattern corresponding to DMPO-X owing to oxidation of DMPO by ROS [51], and even CF also caused a slight signal of DMPO-X. This confirms that ROS shall exist in ACF/CF-mediated oxidation; however, no quartet-like signal of DMPO-OH was observed, suggesting that no significant amount of  $\cdot\text{OH}$  was present.

Furthermore, once 2,2,6,6-Tetramethylpiperidine (TEMP) was adopted as a radical-trapping agent, a distinct pattern of triplet corresponding to TEMPO was detected in both cases of ACF and CF, suggesting that singlet oxygen shall exist and oxidize TEMP to become TEMPO. This result was in line with to the aforementioned result of the effect of radical scavengers. These comparisons also indicate that singlet oxygen shall be present and contribute to VLA oxidation to VAE. This might also provide a possible reason for explaining why the selectivity of VLA to VAE by ACF was relatively high as singlet oxygen is reactive and highly selective [19], but less powerful than free radicals (e.g.,  $\cdot\text{OH}$ ); thus, less over-oxidation and non-selective oxidation of VLA by ACF/CF was observed.

As ACF was also comprised of N, including graphitic N and pyrrolic N species, these N species have been reported to actively participate the oxidation process of alcohols via several possible mechanisms involving reactive oxygen species. First, according to the literature [52], a carbon atom adjacent to a graphitic N atom in a carbonaceous material would be prone to reacting with an oxygen molecule as displayed in Fig. S4(a) (see below) [52]. Subsequently, the oxygen molecule would react with the carbon site and then transfer to several possible intermediates, which would evolve to oxygen radicals for oxidizing alcohols to afford corresponding aldehydes and  $\text{H}_2\text{O}$ . Another previous study has also indicated that carbon materials would mediate the transformation of  $\text{O}_2$  to oxygen radicals (e.g., superoxide), which, however, is unstable, and would then evolve to singlet oxygen up chain reactions with  $\text{H}_2\text{O}$  [53]. On the other hand, oxygen radicals (e.g., superoxide) might be also mediated by catalysts to become singlet oxygen,  $^1\text{O}_2$  [54], which was then detected during VLA oxidation. These resulting reactive oxygen species would be expected to react with

VLA at the alcohol group, which would be then transformed to an aldehyde group, while releasing H<sub>2</sub>O [52].

On the other hand, a previous study reported by Long et al. has also revealed that the N atom of N-doped carbon material might also directly react with O<sub>2</sub> to become an oxidizing intermediate which would then oxidize alcohols to afford aldehydes as depicted in Fig. S4(b) [55]. The presence of DMPO-X might be oxidized by these ROS-containing intermediates present on the surface of ACF. Therefore, the mechanism of VLA conversion to VAE by N-doped ACF might be attributed to ROS-containing intermediates of ACF upon reactions with O<sub>2</sub> molecules.

Besides, one can also notice that the signals of DMPO-X and TEMPO by ACF were more intensive than those by CF, suggesting that ROS generated from ACF seemed much higher than that from CF. Therefore, the conversion efficiency by ACF was noticeably higher than that by CF, possibly because ACF exhibited a significantly higher surface area which enabled ACF to provide more reactive surface for generating ROS and VLA oxidation. Besides, oxygenic functional groups (e.g., carbonyl groups) have been also validated to involve and mediate singlet oxygen-based oxidation processes [16, 18]. Some studies have also observed that singlet oxygen might react with surficial carbonyl groups to become a reactive intermediate for further oxidizing reactions [17]. Since ACF also possessed a higher content of oxygen group (especially carbonyl groups), which might contribute to mediating oxidation processes of singlet oxygen (or other ROS), and even forming other surficial reactive intermediates, thereby enhancing VLA conversion to VAE.

#### 4. Conclusions:

ACF was proposed and demonstrated for the first time as a highly effective heterogeneous catalyst for VLA conversion to VAE without using any metals and oxidizing agents. In comparison to CF, ACF exhibited a surpassingly high surface area and more abundant oxygen functional group, thereby enabling ACF to achieve a much higher conversion of VLA with an ultra-high selectivity towards VAE. At 120 °C within 30 min, ACF could enable  $C_{VLA} = 100\%$  with  $S_{VAE} = 100\%$  in the absence of any metals and oxidants. ACF can be also reused for catalyzing VLA oxidation to VAE over the consecutive five cycles with steady and consistent  $C_{VLA}$  and  $S_{VAE}$ . Via studying the effect of radical scavengers and ESR analyses, the oxidation of VLA to VAE by ACF could be attributed to singlet oxygen via the non-radical route of oxidation, and the higher surface area and abundant carbonyl groups of ACF might provide more reactive surfaces to mediate oxidation processes of VLA, thereby achieving a much higher conversion efficiency. These results confirm that ACF is certainly a promising green heterogeneous catalyst for valorizing VLA into VAE.

#### References:

- [1] R. Yopez, S. Garcia, P. Schachat, M. Sanchez-Sanchez, J.H. Gonzalez-Estefan, E. Gonzalez-Zamora, I.A. Ibarra, J. Aguilar-Pliego, Catalytic activity of HKUST-1 in the oxidation of trans-ferulic acid to vanillin, *New J. Chem.*, 39 (2015) 5112-5115.
- [2] E. Sánchez-González, A. López-Olvera, O. Monroy, J. Aguilar-Pliego, J. Gabriel Flores, A. Islas-Jácome, M.A. Rincón-Guevara, E. González-Zamora, B. Rodríguez-Molina, I.A. Ibarra, Synthesis of vanillin via a catalytically active Cu(ii)-metal organic polyhedron, *CrystEngComm*, 19 (2017) 4142-4146.
- [3] P. Elamathi, M.K. Kolli, G. Chandrasekar, Catalytic Oxidation of Vanillyl Alcohol Using FeMCM-41 Nanoporous Tubular Reactor, *International Journal of Nanoscience*, 17 (2017).

- [4] R. Yepez, J.F. Illescas, P. Gijon, M. Sanchez-Sanchez, E. Gonzalez-Zamora, R. Santillan, J.R. Alvarez, I.A. Ibarra, J. Aguilar-Pliego, HKUST-1 as a Heterogeneous Catalyst for the Synthesis of Vanillin, *J Vis Exp*, (2016).
- [5] J.G. Flores, E. Sánchez-González, A. Gutiérrez-Alejandre, J. Aguilar-Pliego, A. Martínez, T. Jurado-Vázquez, E. Lima, E. González-Zamora, M. Díaz-García, M. Sánchez-Sánchez, I.A. Ibarra, Greener synthesis of Cu-MOF-74 and its catalytic use for the generation of vanillin, *Dalton Transactions*, 47 (2018) 4639-4645.
- [6] M. Fache, B. Boutevin, S. Caillol, Vanillin Production from Lignin and Its Use as a Renewable Chemical, *ACS Sustainable Chemistry & Engineering*, 4 (2016) 35-46.
- [7] P. Elamathi, M.K. Kolli, G. Chandrasekar, Catalytic Oxidation of Vanillyl Alcohol Using FeMCM-41 Nanoporous Tubular Reactor, *International Journal of Nanoscience*, 17 (2018) 1760010.
- [8] S. Saha, S.B. Abd Hamid, Nanosized spinel Cu-Mn mixed oxide catalyst prepared via solvent evaporation for liquid phase oxidation of vanillyl alcohol using air and H<sub>2</sub>O<sub>2</sub>, *RSC Advances*, 6 (2016) 96314-96326.
- [9] S. Saha, S.B.A. Hamid, T.H. Ali, Catalytic evaluation on liquid phase oxidation of vanillyl alcohol using air and H<sub>2</sub>O<sub>2</sub> over mesoporous Cu-Ti composite oxide, *Applied Surface Science*, 394 (2017) 205-218.
- [10] M. Shilpy, M.A. Ehsan, T.H. Ali, S.B. Abd Hamid, M.E. Ali, Performance of cobalt titanate towards H<sub>2</sub>O<sub>2</sub> based catalytic oxidation of lignin model compound, *RSC Advances*, 5 (2015) 79644-79653.
- [11] R. Behling, G. Chatel, S. Valange, Sonochemical oxidation of vanillyl alcohol to vanillin in the presence of a cobalt oxide catalyst under mild conditions, *Ultrason. Sonochem.*, 36 (2017) 27-35.
- [12] K.-Y.A. Lin, H.-K. Lai, Z.-Y. Chen, Selective generation of vanillin from catalytic oxidation of a lignin model compound using ZIF-derived carbon-supported cobalt nanocomposite, *Journal of the Taiwan Institute of Chemical Engineers*, (2017).
- [13] J. Pan, J. Fu, X. Lu, Microwave-Assisted Oxidative Degradation of Lignin Model Compounds with Metal Salts, *Energy & Fuels*, 29 (2015) 4503-4509.
- [14] J.-u. Jang, H.C. Park, H.S. Lee, M.-S. Khil, S.Y. Kim, Electrically and Thermally Conductive Carbon Fibre Fabric Reinforced Polymer Composites Based on Nanocarbons and an In-situ Polymerizable Cyclic Oligoester, *Scientific Reports*, 8 (2018) 7659.

- [15] C.A. Silva, E. Marotta, M. Schuller, L. Peel, M. O'Neill, In-Plane Thermal Conductivity in Thin Carbon Fiber Composites, *J. Thermophys Heat Transfer*, 21 (2007) 460-467.
- [16] C. Felip-León, M. Puche, J.F. Miravet, F. Galindo, M. Feliz, A spectroscopic study to assess the photogeneration of singlet oxygen by graphene oxide, *Mater. Lett.*, 251 (2019) 45-51.
- [17] M. Hajimohammadi, N. Azizi, S. Tollabimazraeno, A. Tuna, J. Duchoslav, G. Knör, Cobalt (II) Phthalocyanine Sulfonate Supported on Reduced Graphene Oxide (RGO) as a Recyclable Photocatalyst for the Oxidation of Aldehydes to Carboxylic Acids, *Catal. Lett.*, 151 (2021) 36-44.
- [18] K. Naim, S.T. Nair, P. Yadav, A. Shanavas, P.P. Neelakandan, Supramolecular Confinement within Chitosan Nanocomposites Enhances Singlet Oxygen Generation, *ChemPlusChem*, 83 (2018) 418-422.
- [19] A. Sagadevan, K.C. Hwang, M.-D. Su, Singlet oxygen-mediated selective C–H bond hydroperoxidation of ethereal hydrocarbons, *Nature Communications*, 8 (2017) 1812.
- [20] G.S. Bhat, R. Schwanke, Thermal properties of a polyimide fiber, *Journal of thermal analysis*, 49 (1997) 399-405.
- [21] A. Li, Z. Ma, H. Song, N. Li, M. Hou, The effect of liquid stabilization on the structures and the conductive properties of polyimide-based graphite fibers, *RSC Advances*, 5 (2015) 79565-79571.
- [22] A. Li, Z.-k. Ma, H.-h. Song, K. Lu, Z.-j. Liu, Q.-g. Guo, Effect of heat treatment temperature on the microstructure and properties of polyimide-based carbon fibers, *Carbon*, 85 (2015) 447.
- [23] M. Xiao, N. Li, Z. Ma, H. Song, K. Lu, A. Li, Y. Meng, D. Wang, X. Yan, The effect of doping graphene oxide on the structure and property of polyimide-based graphite fibre, *RSC Adv*, 7 (2017) 56602-56610.
- [24] T. Lee, C.-H. Ooi, R. Othman, F.-Y. Yeoh, ACTIVATED CARBON FIBER - THE HYBRID OF CARBON FIBER AND ACTIVATED CARBON, in, 2014.
- [25] A. Clearfield, M.E. Kuchenmeister, K. Wade, R. Cahill, P. Sylvester, Pillaring of Layered Inorganic Compounds: Fundamentals, in: M.L. Occelli, H.E. Robson (Eds.) *Expanded Clays and Other Microporous Solids*, Springer US, Boston, MA, 1992, pp. 245-262.
- [26] S. Fu, Q. Fang, A. Li, Z. Li, J. Han, X. Dang, W. Han, Accurate characterization of full pore size distribution of tight sandstones by low-temperature nitrogen gas adsorption and high-pressure mercury intrusion combination method, *Energy Science & Engineering*, 9 (2021) 80-100.

- [27] A. Jha, K. Patil, C. Rode, Mixed Co–Mn Oxide-Catalysed Selective Aerobic Oxidation of Vanillyl Alcohol to Vanillin in Base-Free Conditions, *ChemPlusChem*, 78 (2013).
- [28] S. Ramana, B.G. Rao, P. Venkataswamy, A. Rangaswamy, B.M. Reddy, Nanostructured Mn-doped ceria solid solutions for efficient oxidation of vanillyl alcohol, *J. Mol. Catal. A: Chem.*, 415 (2016) 113-121.
- [29] S.R. Kubota, K.S. Choi, Electrochemical Oxidation of 5-Hydroxymethylfurfural to 2,5-Furandicarboxylic Acid (FDCA) in Acidic Media Enabling Spontaneous FDCA Separation, *ChemSusChem*, 11 (2018) 2138-2145.
- [30] K.-Y.A. Lin, J.-T. Lin, X.-Y. Lu, C. Hung, Y.-F. Lin, Electrospun magnetic cobalt-embedded carbon nanofiber as a heterogeneous catalyst for activation of oxone for degradation of Amaranth dye, *Journal of Colloid and Interface Science*, 505 (2017) 728-735.
- [31] K.-Y.A. Lin, M.-T. Yang, J.-T. Lin, Y. Du, Cobalt ferrite nanoparticles supported on electrospun carbon fiber as a magnetic heterogeneous catalyst for activating peroxymonosulfate, *Chemosphere*, 208 (2018) 502-511.
- [32] G. Li, J. Sun, W. Hou, S. Jiang, Y. Huang, J. Geng, Three-dimensional porous carbon composites containing high sulfur nanoparticle content for high-performance lithium–sulfur batteries, *Nature Communications*, 7 (2016) 10601.
- [33] L. Lu, Q. Hao, W. Lei, X. Xia, P. Liu, D. Sun, X. Wang, X. Yang, Well-Combined Magnetically Separable Hybrid Cobalt Ferrite/Nitrogen-Doped Graphene as Efficient Catalyst with Superior Performance for Oxygen Reduction Reaction, *Small*, 11 (2015) 5833-5843.
- [34] J. Liu, T. Zhang, Z. Wang, G. Dawson, W. Chen, Simple pyrolysis of urea into graphitic carbon nitride with recyclable adsorption and photocatalytic activity, *J. Mater. Chem.*, 21 (2011) 14398-14401.
- [35] X. Ma, H. Yang, L. Yu, Y. Chen, Y. Li, Preparation, Surface and Pore Structure of High Surface Area Activated Carbon Fibers from Bamboo by Steam Activation, *Materials*, 7 (2014) 4431-4441.
- [36] Y. Guo, S. Wang, K. Ruan, H. Zhang, J. Gu, Highly thermally conductive carbon nanotubes pillared exfoliated graphite/polyimide composites, *npj Flexible Electronics*, 5 (2021) 16.
- [37] J.-Y. Lin, J. Lee, K.-Y.A. Lin, Microwave-Assisted Catalyst-Free Oxidative Conversion of a Lignin Model Compound to Value-Added Products Using TEMPO, *Waste and Biomass Valorization*, 11 (2020) 3621-3628.
- [38] Z.M.A. Bundhoo, Microwave-assisted conversion of biomass and waste materials to biofuels, *Renewable and Sustainable Energy Reviews*, 82 (2018) 1149-1177.

- [39] P. Chen, Q. Xie, Z. Du, F.C. Borges, P. Peng, Y. Cheng, Y. Wan, X. Lin, Y. Liu, R. Ruan, Microwave-Assisted Thermochemical Conversion of Biomass for Biofuel Production, in: Z. Fang, J.R.L. Smith, X. Qi (Eds.) Production of Biofuels and Chemicals with Microwave, Springer Netherlands, Dordrecht, 2015, pp. 83-98.
- [40] Z. Zhang, Z.K. Zhao, Microwave-assisted conversion of lignocellulosic biomass into furans in ionic liquid, *Bioresour Technol*, 101 (2010) 1111-1114.
- [41] C. Li, Z. Zhang, Z.K. Zhao, Direct conversion of glucose and cellulose to 5-hydroxymethylfurfural in ionic liquid under microwave irradiation, *Tetrahedron Lett.*, 50 (2009) 5403-5405.
- [42] D. Gunwant, A. Vetrnam, Microwave absorbing properties of carbon fiber based materials: A review and prospective, *Journal of Alloys and Compounds*, 881 (2021) 160572.
- [43] N. Zhao, T. Zou, C. Shi, J. Li, W. Guo, Microwave absorbing properties of activated carbon-fiber felt screens (vertical-arranged carbon fibers)/epoxy resin composites, *Materials Science and Engineering: B*, 127 (2006) 207-211.
- [44] W. Ye, W. Li, Q. Sun, J. Yu, Q. Gao, Microwave absorption properties of lightweight and flexible carbon fiber/magnetic particle composites, *RSC Advances*, 8 (2018) 24780-24786.
- [45] B. Rahmanivahid, M. Pinilla-de Dios, M. Haghghi, R. Luque, Mechanochemical Synthesis of CuO/MgAl<sub>2</sub>O<sub>4</sub> and MgFe<sub>2</sub>O<sub>4</sub> Spinel for Vanillin Production from Isoeugenol and Vanillyl Alcohol, *Molecules*, 24 (2019).
- [46] R. Behling, G. Chatel, S. Valange, Sonochemical oxidation of vanillyl alcohol to vanillin in the presence of a cobalt oxide catalyst under mild conditions, *Ultrason Sonochem*, 36 (2017) 27-35.
- [47] S. Saha, S.B.J.R.a. Abd Hamid, Nanosized spinel Cu–Mn mixed oxide catalyst prepared via solvent evaporation for liquid phase oxidation of vanillyl alcohol using air and H<sub>2</sub>O<sub>2</sub>, 6 (2016) 96314-96326.
- [48] S. Saha, S.B. Abd Hamid, T.H.J.A.S.S. Ali, Catalytic evaluation on liquid phase oxidation of vanillyl alcohol using air and H<sub>2</sub>O<sub>2</sub> over mesoporous Cu-Ti composite oxide, 394 (2017) 205-218.
- [49] M.-W. Zheng, H.-K. Lai, K.-Y.A. Lin, Valorization of Vanillyl Alcohol by Pigments: Prussian Blue Analogue as a Highly-Effective Heterogeneous Catalyst for Aerobic Oxidation of Vanillyl Alcohol to Vanillin, *Waste and Biomass Valorization*, 10 (2019) 2933-2942.
- [50] K. Bao, F. Li, H. Liu, Z. Wang, Q. Shen, J. Wang, W. Zhang, Activated carbon for aerobic oxidation: Benign approach toward 2-benzoylbenzimidazoles and 2-benzoylbenzoxazoles synthesis, *Scientific Reports*, 5 (2015) 10360.

- [51] P. Bilski, K. Reszka, M. Bilska, C.F. Chignell, Oxidation of the Spin Trap 5,5-Dimethyl-1-pyrroline N-Oxide by Singlet Oxygen in Aqueous Solution, *J. Am. Chem. Soc.*, 118 (1996) 1330-1338.
- [52] H. Watanabe, S. Asano, S.-i. Fujita, H. Yoshida, M. Arai, Nitrogen-Doped, Metal-Free Activated Carbon Catalysts for Aerobic Oxidation of Alcohols, *ACS Catal*, 5 (2015) 2886-2894.
- [53] X. Dou, Z. Lin, H. Chen, Y. Zheng, C. Lu, J.-M. Lin, Production of superoxide anion radicals as evidence for carbon nanodots acting as electron donors by the chemiluminescence method, *Chem. Commun.*, 49 (2013) 5871-5873.
- [54] Q. Yi, J. Ji, B. Shen, C. Dong, J. Liu, J. Zhang, M. Xing, Singlet Oxygen Triggered by Superoxide Radicals in a Molybdenum Cocatalytic Fenton Reaction with Enhanced REDOX Activity in the Environment, *Environ. Sci. Technol.*, 53 (2019) 9725-9733.
- [55] J. Long, X. Xie, J. Xu, Q. Gu, L. Chen, X. Wang, Nitrogen-Doped Graphene Nanosheets as Metal-Free Catalysts for Aerobic Selective Oxidation of Benzylic Alcohols, *ACS Catal*, 2 (2012) 622-631.